

RINGSS turbulence sensor based on Celestron Nexstar 5SE

Authors: *A. Tokovinin*

Version: 1

Date: 2021-03-30

File: prj/smss/doc/RINGSS-Celestron.tex

1 Introduction

RINGSS is a turbulence monitor based on the analysis of defocused image of a bright single star in a small telescope (Tokovinin, 2021). The concept can be implemented using various optical solutions. Here a particular realization based on the commercial amateur telescope Celestron Nexstar 5SE (hereafter Celestron) is described. This telescope was chosen for its compactness (tube length 270mm, tube diameter 150mm, mass 2.35kg). Size is an important consideration for a portable site-testing instrument.

This document covers various aspects of using Celestron in RINGSS: the design of the coupling optics, its implementation and test, focusing, and mechanical interface.

2 Optical Coupling

2.1 Optical Requirements

The optics of RINGSS must form a ring-like image of a point source, hence the wavefront shape must be conic. This is achieved by a combination of defocus and spherical aberrations in a 1:10 proportion and with opposite signs. The curvature of a defocused (spherical) wavefront is compensated by the spherical aberration, resulting in a very good approximation of the conic wavefront. The amount of spherical aberration is fixed by the optics, so, for a given instrument, there is an optimum defocus. This defocus must correspond to the conjugation distance of ~ 0.5 km below ground.

The second requirement is the short effective focal length F of ~ 0.4 m to provide the desired pixel scale of $1.5''$ using a CMOS camera ZWO ASI290 with a small pixels of $2.9 \mu\text{m}$. A shorter focal distance would under-sample the ring in the radial direction, while a much longer F would decrease the flux per pixel and the S/N ratio.

Both requirements are fulfilled by reducing the native focal length of the telescope, $F = 1250$ mm, with a positive lens in front of the camera. A custom lens design can provide the desired amount of spherical aberration and correct the chromatism. Here, the same goal is achieved by a combination of two off-the-shelf lenses. If just one standard achromatic doublet is used as a focal reducer, its under-corrected spherical aberration is exploited, but its under-corrected chromatism remains.

It is instructive to evaluate the reduction of the effective focal distance using the thin-lens formula. If f is the lens focal distance and l the distance from the lens to the camera, the reduction factor k is

$$k = f/(f - l), \tag{1}$$

provided that $l < f$. The distance from the original focus to the lens is simply kl . With l increasing and approaching f , the reduction factor can take large values, and the original focus will be at a large distance behind the lens, tending to infinity. Large values of k are associated with large aberrations. For the Celestron, the de-magnification factor must be large, $k = 1250/350 \approx 3.6$. The aberrations are also large, which forces to use a lens with a short focal distance f to decrease the beam footprint on the lens.

2.2 Optical design

The optical prescriptions of the Celestron telescopes are a commercial secret of the vendor. The starting point of the present design is an equivalent Richey-Cretien 2-mirror reflector that matches the actual telescope approximately. Based on the dimensions of the telescope, I select the primary mirror M1 of $D = 125$ mm diameter with a curvature radius of 435 mm and a concave secondary mirror M2 with a radius of 163 mm placed at a distance of 163 mm in front of the primary. The image plane is at 150 mm behind the primary (this distance is poorly known and only approximate). The conic constant of M2 is -3.0 , and the conic constant of M1 is adjusted to -1.1382 to get a stigmatic on-axis image. The effective focal length $F = 1248$ mm matches the nominal F/10. This equivalent design is `Celestron5SE.zmx`. The aperture is masked to the central obscuration of 0.5 (it is 0.39 in the native telescope, but should be 0.5 in RINGSS).

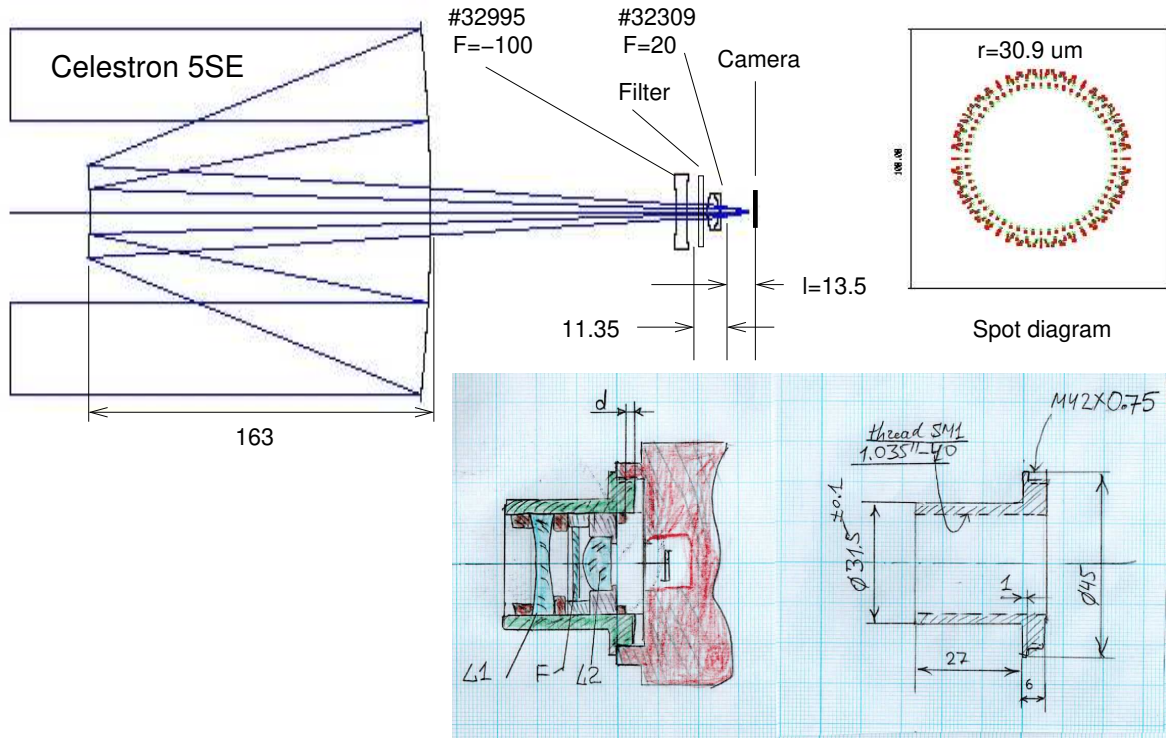


Figure 1: Optical layout and spot diagram. The blue, red, and green colors in the spot diagram denote wavelengths of 0.5, 0.6, and 0.7 μm . The sketches below show the mechanical adapter.

Table 1: Main optical parameters

Element	Parameters	Dist. next	Comment
Primary M1	$R = 435$, $CC = -1.1382$	-163	Moves to adjust focus
Secondary M2	$R = -132$, $CC = -3.0$	163+120	Fixed
Negative lens L1	$F = -100$, $D = 25$	~ 12	EO #32995, #47-919
Achromat L2	$F = 20$, $D = 12.5$	13.5*	EO #32309, #47-661
Camera	pixel $2.9 \mu\text{m}$	0	Focal plane

The optical design described here, `Celestron5SE-L20bb.zmx`, is illustrated in Figure 1. It uses commercial lenses from Edmund Optics, namely the achromatic doublet #32309 (diam. 12.5 mm, $f = 20$ mm) and the negative bi-convex lens #32995 (diam. 25 mm, $f = -100$ mm). The negative lens is needed to correct the residual chromatism. The distance between the lenses is not critical, but smaller values are preferable to reduce the vignetting.

The adjustable parameter of this design is the distance between the last lens and the camera, which we call l in analogy with the thin-lens formula (1). With increasing l , the de-magnification factor k becomes larger, the beam footprint on the lens increases, and the residual spherical aberration a_{11} also increases. With $l = 13.5$ mm, the effective focal length is 423 mm (slightly longer than optimum) and the pixel scale is $1.41''$. The beam diameter on the lens is ~ 5 mm, and the spherical aberration is $a_{11} = 0.19$. A conic wavefront is reached by moving the camera+lenses assembly forward by 3 mm (then $a_4 = 1.92$), which corresponds to the conjugation distance of 520 m. The resulting ring image, shown in Fig. 1, has a geometric radius of $30.9 \mu\text{m}$, or about 11 pixels.

By moving the lenses further away from the camera by 0.5 mm (to $l = 14$ mm), we would reduce the effective focal distance to 407 mm. The spherical aberration increases to $a_{11} = 0.234$, and a conic wavefront is obtained for a 4-mm defocus. The ring radius increases to $41.2 \mu\text{m}$.

The optical design is based on the fiducial telescope model. The real telescope is slightly different. Some adjustment of the effective focal length, pixel scale, and optimum defocus can be achieved by a suitable choice of l . The actual lenses ordered for the instrument have a VIS-0° coating (EO parts #47-919, #47-661). The main parameters of the optics are listed in Table 1. To complement them, the spectral filter FES0750 was ordered from Thorlabs. It transmits wavelengths from 500 to 750 nm with an almost rectangular response curve and the maximum transmission of 0.90, limited mostly by the reflection losses. This filter has a parasitic transmission around 400 nm that can be blocked by a yellow filter (e.g. FGL455 from Thorlabs). However, at present the blocking filter is not used.

Figure 1 shows the sketch of the mechanical adapter holding the optics. It couples to the camera by the M42×0.75 metric thread. The outer diameter of 31.5 mm matches standard eyepieces, allowing to clamp the holder in the Celestron’s adapter. The internal thread of Thorlabs SM-1 standard allows us to use commercial elements, namely two retaining rings and the $0.5''$ lens holder for L2. The critical distance $l = 13.5$ mm is regulated by setting the inner ring edge at $d = 3$ mm inside the adapter. Given that the CMOS is located at 12.5 mm depth from the camera flange, this setting corresponds to the nominal l because the back surface of L1 is at 1 mm outside the camera flange. The filter F is located between the lenses; a plastic spacer separates it from L1.

The telescope central obscuration is set to 0.5 by clamping an annular cardboard mask with an outer diameter of 63 mm to the protruding end of the secondary mirror unit (diameter 49 mm).

2.3 On-sky optics test

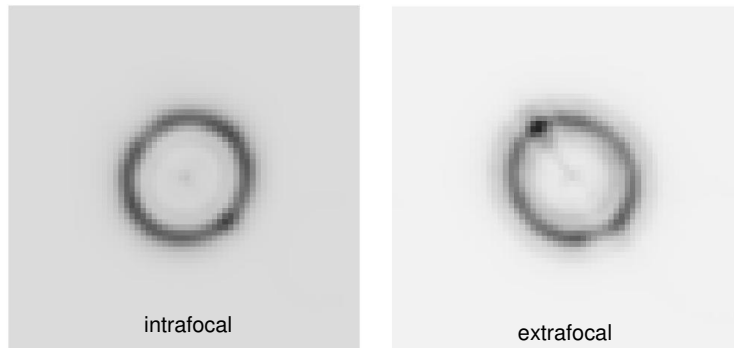


Figure 2: Average ring images recorded on 2021-03-21. Left: Sirius, intrafocal, $r = 11.2$ pixels, sharp ring; right: Procyon, extrafocal, $r = 11.05$ pixels, fuzzy ring. The image size is 64×64 pixels.

Given that the telescope prescription used in the optical design is only a guess, it is essential to test the actual instrument on the sky. The pixel scale was measured on 2021-02-19 by taking images of three wide double stars with separations from $69''$ to $241''$. All three pairs gave a consistent result: the pixel scale is $1.43'' \pm 0.01''$. It matches very well the optical design.

Figure 2 shows average ring images obtained from the 2-s image cubes by the IDL pipeline. The data were taken on 2021-03-21. When the focus setting corresponds to the nominal ring radius around 10 pixels, the pipeline measures the ring width of 2.8 pixels which matches the expected diffraction-limited width within 10%. Therefore, the optics works as designed. For comparison, this Figure shows the extra-focal ring of the same radius where the spherical aberration and defocus have the same signs and, instead of producing a conic wavefront, give a fuzzy ring image.

One can note that the rings are slightly elongated. This indicates a small astigmatism. The astigmatism is caused by the imperfect lens centering. It depends on the source position in the field; by selecting a slightly de-centered ROI, one can eliminate the astigmatism, should this be necessary. Another notable feature is a bright knot and a dimming opposite to it. This feature changes its orientation between intrafocal and extrafocal images. It is most likely caused by the local distortion of the primary mirror; it was noted in the earlier tests of this telescope using different, provisional lenses.

3 Focusing

The Celestron telescope is focused by moving its primary mirror. The focus range is very large. Such focusing is typical for amateur Schmidt-Cassegrain telescopes. Often the focusing causes tilts of the primary mirror affecting the pointing. However, in this telescope the focusing knob actuates very smoothly, without backlash or tilts. Therefore, it is preferable to use this native focus mechanism instead of installing additional focuser. Tests have shown that telescope orientation does not change the ring radius (less than 0.5 pixel effect).

Preliminary tests of the focus mechanism indicate that the knob rotation by 1 degree changes the ring radius by ~ 0.5 pixels. To maintain constant ring radius in spite of temperature changes, the knob

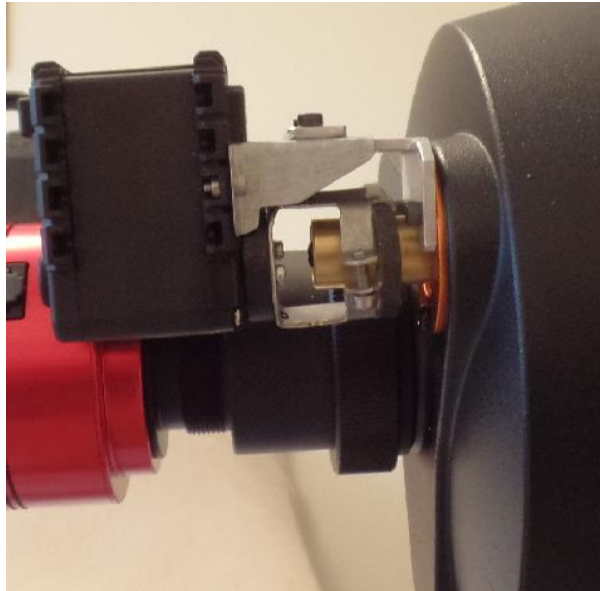


Figure 3: Coupling of the AX-12A servo motor to the focus knob.

will be turned only by several degrees. By turning the knob counterclockwise, we move the focal plane out (away from the primary mirror). For the normal (intrafocal) case, this increases the ring radius.

There are several commercial solutions for remote focus control used by amateurs; in some of them, a motor is attached to turn the focus knob under remote control. However, all commercial focusers are too large for a 5" telescope and would not fit. We will use instead a compact servo motor AX-12A from Dynamixel to control the focus knob remotely. The motor axis can turn by 300° with a step of 0.3° . The motor does not need initialization. It is controlled by a 3-line interface which is driven from a computer through a USB port.

Figure 3 shows a photo of the motor coupling. To allow for the mismatch between the knob and motor's axes, the motor is connected via a flexible clamp with rubber pads. An aluminum bracket bolted to the focus knob base holds the motor, which is easily removable. The idea is to focus the telescope manually and then to attach and clamp the motor (in the middle of its working range) for remote focus control.

References

Tokovinin A., 2021, MNRAS, 502, 794